CHAPTER 7
CASE STUDIES

7.1 INTRODUCTION

The following two case studies demonstrate attempts to confirm the models that were developed for purposes of evaluating stope support, and examples whereby the principles given in this research are tested. The study demonstrates the stable- and unstable failure of stope support.

Both the case studies were carried out at Beatrix Gold Mine. The mine is situated on the southern brim of the Free State Gold Field and is considered to be a shallow to intermediate depth mining operation.

The Beatrix Reef that is mined is the major gold bearing horizon and occurs as the basal conglomerate of a channel deposit at or near the base of the Turffontein Sub Group in the area. This channel deposit is correlated with the Aandenk Channel of the formation as developed on St Helena and Unisel Mines. The reef channel width varies from 20 cm to as much as 7 m and consists of a multi-cycle upwards fining sequence of poorly sorted conglomerates and quartzite. The overall gold mineralisation is generally very high in the wide channels and lower grades are encountered in the narrower channels. The reef sub-outcrops at approximately 800 m below surface. Mining depth varied at the time of the study from 800 m to approximately 950 m below surface. The general strike direction of the reef is north-south while the reef dip varies from near vertical in the vicinity of the western basin edge over-fold to an estimated 5 degrees in the east.

The hangingwall of the Beatrix Reef is a competent quartzite and can be described as massive with well-defined parting planes. The uniaxial compressive strength of the hangingwall ranges from 190 – 220 MPa. The footwall may be considered as weak with a uniaxial compressive strength of approximately 160 MPa. In-situ measurements confirmed a horizontal to vertical virgin stress ratio of 1.

In the first case study namely the 15A47 Stope unstable failure of the supports occurred whereas stable failure of the supports occurred in the second case study namely the 23A79 Stope.

A number of stope panel collapses occurred on the mine in the early 1980's. After these collapses it became a common strategy on the mine to instrument stope

panels with the objective to identify abnormally high closure rate panels on the mine. This formed part of the mine's policy to timeously identify these potentially unstable panels. The majority of the stopes were therefore instrumented at the time of the study as part of this pro-active safety policy on the mine.

7.2 CASE STUDY 1: 15A47 STOPE – UNSTABLE SUPPORT FAILURE

7.2.1 Support capacity

The 15A47 was one of the stopes that was instrumented and where a major collapse of the stope occurred. Nobody was injured during this incident as the systematic stope closure measurements indicated accelerated stope closure prior to the collapse and all workers were prohibited from entering the working place. This incident became an ideal case study to apply and confirm the rockmass stiffness principles that were developed.

The 15A47 Stope was supported by means of an end-grained type of timber pack that will be called the Beatrix End-grain pack in this document. The term end-grain is defined in Chapter 9 of this document. The pack shows a steady increase in the load generated by it as deformation takes place. It was only after the stope collapsed and the support units were tested to destruction that the strain softening behaviour of the pack was identified for the first time. The mathematical representation of the load deformation performance curve for the Beatrix End-Grain pack is shown in Figure 7.1. The constants of the polynomial that quantifies its capacity are listed in Table 4.2 in Chapter 4.

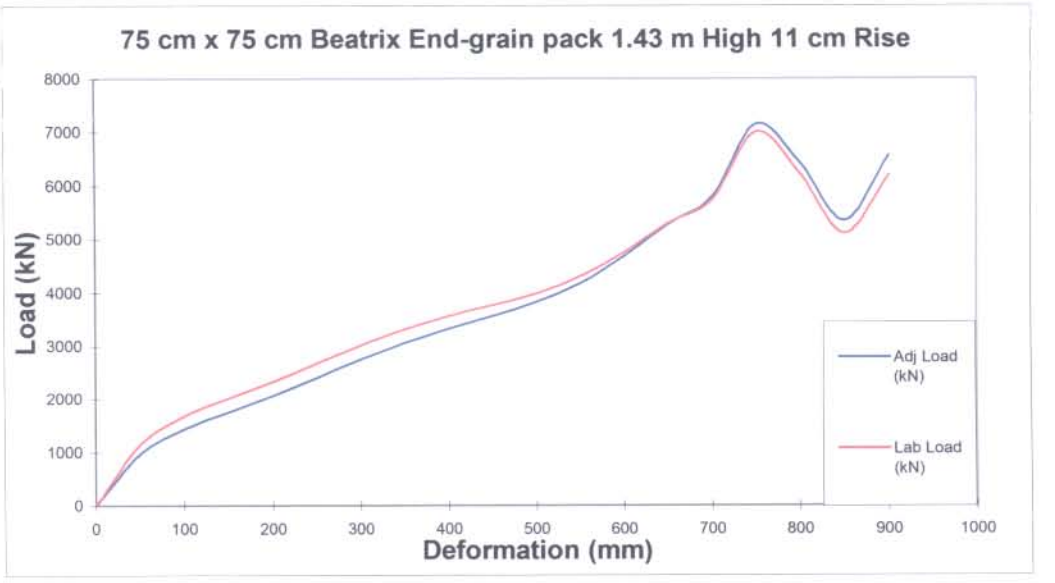

Figure 7.1: Load-deformation curve of Beatrix end-grained pack used in the 15A47 Stope

7.2.2 Rockmass demand

The different stages of mining of the 15A47 Stope as well as the positions of the measuring stations are shown on the plan in Figure 7.2. It also shows the pillar towards the centre of the stope that was left and that acted as regional support. The numbers and the positions of the measuring stations are also shown. The dip of the reef in this area is approximately 12° with the dip direction shown.

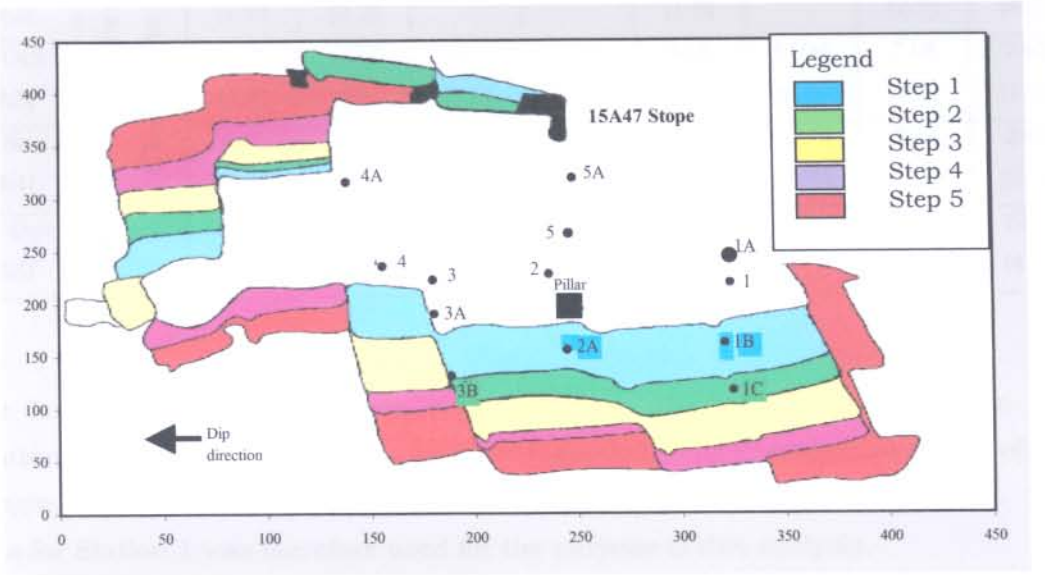

Figure 7.2: Layout and mining steps of the 15A47 Stope

Table 7.1 gives a summary of the stope closure measurements and stope closure rates of reliable stations for the last 5 mining stages (A1 to A5) before the stope collapsed. Reliable stations refer to stations where it was considered that the data obtained was not influenced by human error or where the pegs were replaced at some later stage due to damage or loss of the pegs as a result of the blasting or cleaning operations.

Where no values are given in the tables below it is due to the fact that the station was either:

* not installed at that stage of mining, or

** where the measuring station was lost.

Table 7.1: Summary of closure and closure rates for 15A47 Stope

Date (Mining Stage)	Measuring Station								
	Closure (mm) (Closure rate (mm/day))	1	1A	1B	1C	2	2A	3A	5
16 Aug (A1)		400	90	*	*	345	*	588	165
6 Sept (A2)		439 (1.9)	95 (0.2)	113	*	384 (1.9)	1184	644 (2.7)	205 (4.8)
6 Oct (A3)		488 (1.6)	100 (0)	162 (1.6)	302	446 (2.1)	1194 (0.4)	718 (2.5)	240 (1.2)
9 Nov (A4)		623 (4.0)	100 (0)	368 (6.1)	502 (5.9)	593 (4.3)	1274 (2.4)	893 (5.1)	349 (3.2)
26 Dec (A5)		779 (3.3)	100 (0)	600 (4.9)	800 (6.3)	**	**	1140 (5.3)	555 (4.4)

The last closure measurements were taken on the 26th December when the continued acceleration in closure rate was identified. The first signs of failure of the hangingwall beam started to occur in the area of measuring Station Number 1. The data for Station 1 was therefore used for the purpose of this analysis.

The Attributed area (A_a) was determined for each of the measuring stations for all the mining steps according to the methodology described in Chapter 5. The Attributed areas for each of the measuring stations at the different mining intervals are given in Table 7.2.

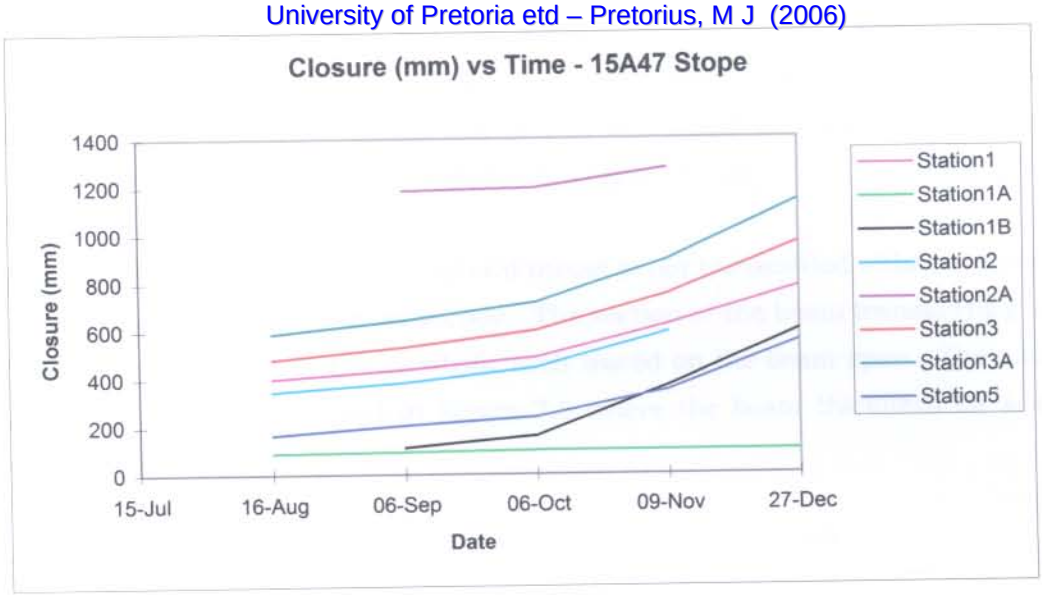

Figure 7.3: Stope closure at the measuring stations – 15A47 Stope

The stope closure of the measuring stations for the 5 stages of mining of the 15A47 Stope is shown in Figure 7.3. The accelerated closure prior to the collapse of the stope is demonstrated where this was common to all the measuring stations accept Station 1A. The hangingwall beam sheared in close proximity to station 1A and the measuring station never registered any closure for this reason.

Table 7.2: Attributed areas for measuring stations – 15A47 Stope

Date (Mining Stage)	Measuring Station								
	Attributed area (m^2)	1	1A	1B	1C	2	2A	3A	5
16 Aug (A1)		1771	1815	*	*	1973	*	1060	2156
6 Sept (A2)		1822	1885	1830	*	1978	1194	1301	2200
6 Oct (A3)		1884	1986	1985	1585	2212	1595	1568	2257
9 Nov (A4)		1910	2087	2124	1819	2400	1652	1883	2315
26 Dec (A5)		2596	2555	2500	2176	**	**	2618	2693

A Voussoir Beam study was done by Kotzé (1991) for Beatrix Mine to determine stable spans for varying beam thicknesses. The design procedure is based on the voussoir beam model for a roof bed and is illustrated in Figure 7.4(a) while the forces operating in the system are defined in Figure 7.4(b).

In the equilibrium condition, the lateral thrust is not transmitted either uniformly or axially through the beam cross section. The section of the beam transmitting lateral load is approximated by the parabolic arch traced on the beam span. The outcome of this study is summarised in Figure 7.5 where the beam thickness for a stable span is plotted.

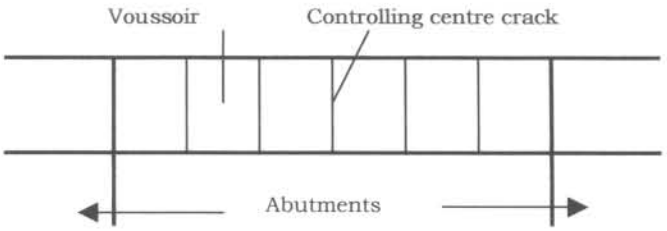

Figure 7.4(a): Voussoir beam model for a roof bed after Kotzé (1991)

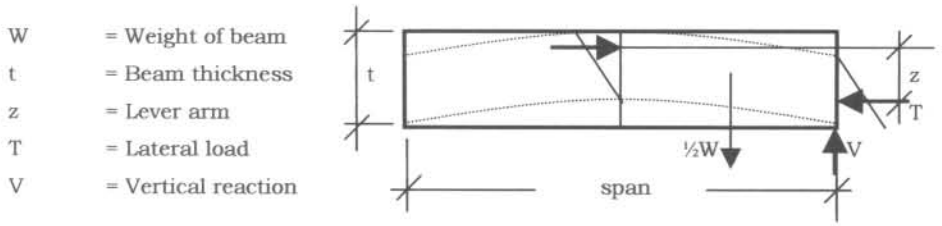

Figure 7.4(b): Forces operating in Voussoir beam system

The mining span between regional supports was 65 m at the time that failure started to occur. This relates to a beam thickness of 8 m. A beam thickness of 8 m was thus accepted for the purpose of this study.

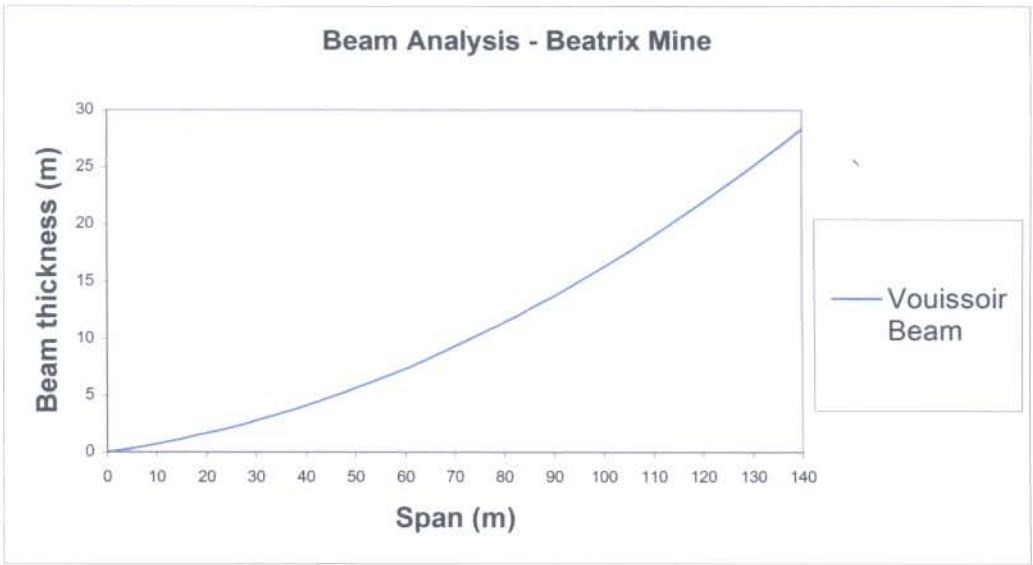

Figure 7.5: Voussoir beam analysis for Beatrix Mine after Kotzé (1991)

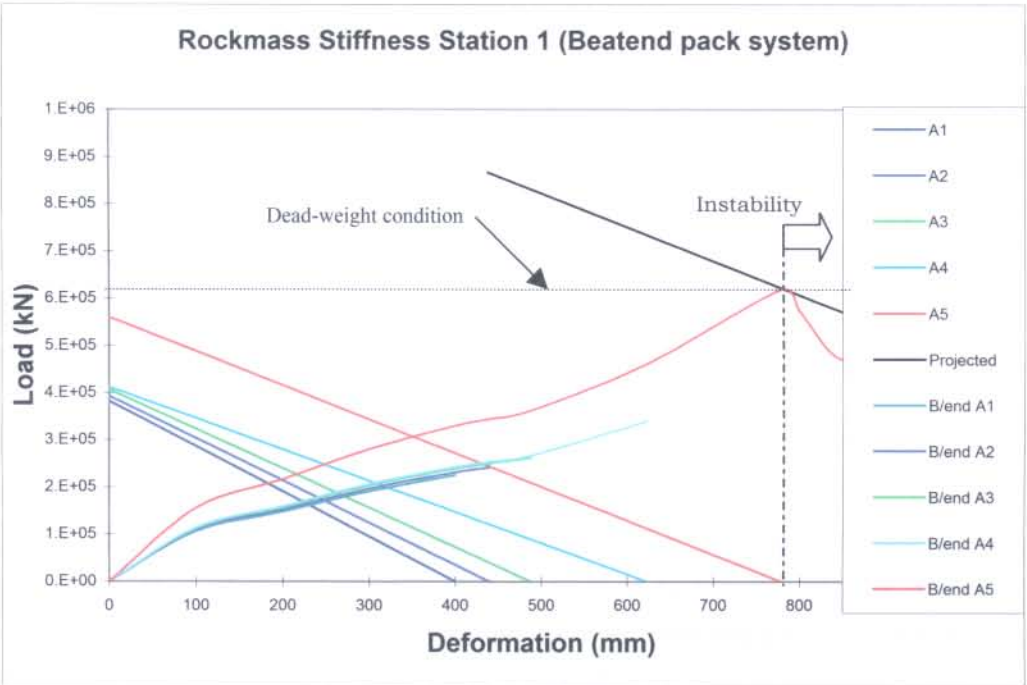

Figure 7.6: Rockmass-support interaction for the 15A47 Stope

Figure 7.6 shows the rockmass/support interaction for the 15A47 stope during five stages of mining denoted by A1 to A5. The analysis illustrates how the stiffness of the rockmass changes as the mining span increases with the consecutive mining steps. The slope of the line representing rockmass stiffness decreases and the rockmass thus reacts in a softer fashion as shown in Table 7.3. This study confirms

the statement made by Ozbay and Roberts (1988) that the rockmass stiffness is related to the mining span.

The force generated by the support system, comprising Beatrix end-grained packs is shown in Figure 7.6. This force that is calculated for the consecutive mining steps takes into account all the factors that influence the support performance as described in Chapter 4. For the purpose of the analysis the actual closure rate for the different stages of mining with support spacing of 3 m (on dip) by 4 m (on strike) were used, with no pre-stressing of the supports.

The area totally collapsed after the fifth stage of mining and closure measurements were therefore only taken up to the fifth stage of mining, i.e. up to 779 mm of stope closure. The excavation was stable during these five stages of mining.

The support system started failing after the fifth stage of mining where the energy released by the rockmass exceeds that generated by the support system as given in Table 7.3. The last stage of mining (denoted by "projected") is a prediction of strata stiffness assuming that total closure has taken place. The projected line representing the rockmass stiffness as post stage 5 of mining is assumed to be parallel to that of mining stage A5. A more conservative approach to this would have been to represent rockmass stiffness with a horizontal line where this option would have represented a dead-weight condition of the hangingwall rockmass.

(a) Stability analysis

The rockmass stiffness and the energy generated and absorbed by the rockmass and supports respectively for the 5 mining steps of measuring Station 1 is summarised in Table 7.3. It shows the stiffness and energy for both the rockmass and the supports for the different intervals of deformation during the mining stages. For purposes of the analysis the calculations were extrapolated for a "Post A5" stage where entry into the working place was not possible.

Examples of the stability analysis calculations are shown as Appendix 1 at the end of the chapter.

Table 7.3: Stability analysis summary for Station 1

Mining Stage	Deform. interval (mm)	Stiffness (kN/mm)		Energy (kJ) for mining stage		Comment
		Rockmass	Supports	Released by the Rockmass	Absorbed by the Supports	
A1	0-400	-956	+ 516	70443	71806	Stable
A2	400-439	-896	+ 318	681	11057	Stable
A3	439-488	-833	+ 335	1005	14911	Stable
A4	488-623	-662	+ 680	6029	50723	Stable
A5	623-779	-719	+ 6149	8751	108594	Stable
Post A5	779-900	-719	-1209	85038	62617	Unstable failure of supports

The analysis shows that the energy released by the rockmass for the different intervals of deformation at Station 1 prior to failure (Mining Stages A1 to A5) is less than the energy absorbed by the supports. Once the deformation value of 779 mm is exceeded (Post A5 Mining Stage), the energy released by the rockmass exceeds the capacity of the supports, and unstable failure of the supports occurs. The energy released by the rockmass in mining stage post A5 is 85038 kJ as opposed to the 62617 kJ absorbed by the supports during the deformation interval 779 - 900 mm.

The rockmass stiffness has negative slope for the first 5 mining stages while that of the supports are positive for the same five stages of mining. For the mining stage post A5 the slope of the rockmass is less than the supports and indicates unstable support failure. The stiffness of the rockmass for this deformation interval is –719 kN/mm as opposed to the –1209 kN/mm of the support.

This approach validates the evaluation methodology from both stiffness and energy comparison points of view. The study confirms that the instability could gave originated in the vicinity of Station 1 as was observed underground.

7.3 CASE STUDY 2: 23A79 STOPE – STABLE SUPPORT FAILURE

After the stope collapse of the 15A47 Stope, a decision was taken by management on the mine to introduce a systematic pillar layout as regional support. The objective of this strategy was to limit the mining span and through this limit stope closure. The effect of this strategy was that it would in turn affect the stiffness of the rockmass. After some experimental stopes it was decided to use Pencil Props as permanent stope panel support with Matpacks as gully support.

The mining depth of the 23A79 Stope is approximately 800 m below surface. Regional support in the form of 6 m x 3 m pillars were introduced in this area as part of the mine's strategy. In practice the pillars were cut slightly larger than was required after the 4th stage of mining as shown in Figure 7.8.

7.3.1 Support capacity

The mathematical representation of load-deformation performance curves for a Profile Prop and a Matpack that were used in the 23A79 Stope is shown in Figures 7.7 and 7.8. The graphs represent the in-situ performance of the support units installed in the 23A79 Stope where the laboratory test results were adjusted to compensate for the factors influencing its performance. The rate of deformation for each of the mining steps was taken as determined from the in-situ measurements shown in Table 7.4. The support units were not pre-stressed during installation.

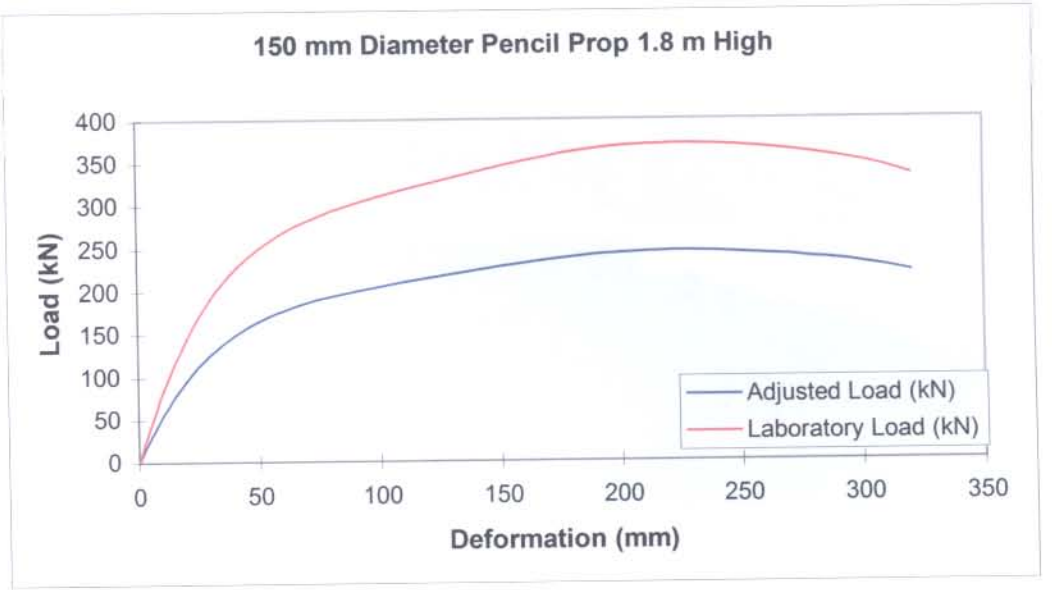

Figure 7.7: Load–deformation curve for a 150 mm Diameter Pencil Prop used in the 23A79 Stope

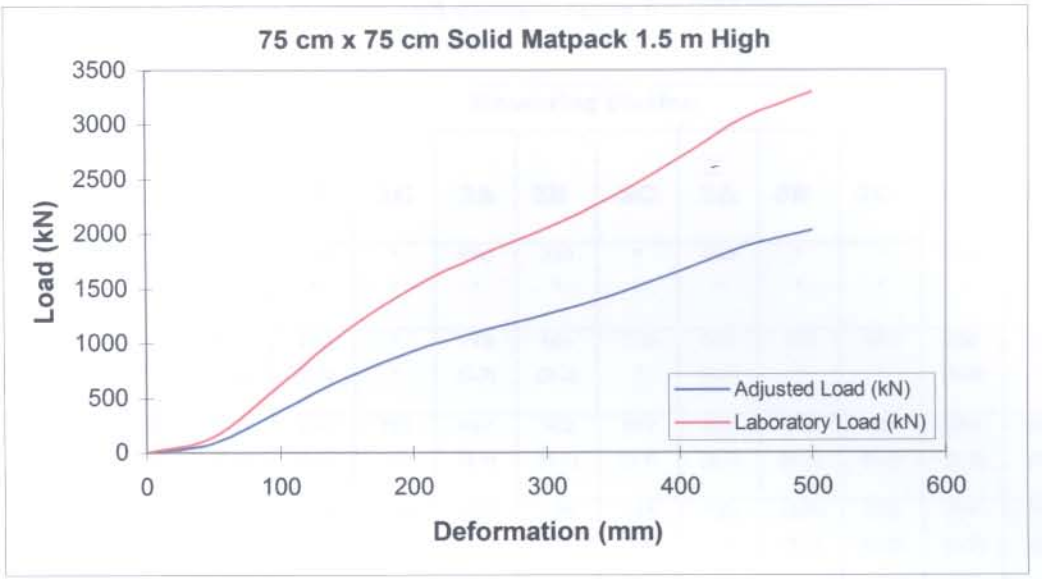

Figure 7.8: Load–deformation curve for a 75 cm x 75 cm Matpack used in the 23A79 Stope

7.3.2 Rockmass demand

The mining steps during the five stages of mining of this working place is shown in Figure 7.9. The dip-oriented pillars can be seen where these were introduced after the 4th mining stage. The effect that the pillars have on the measurements in this stope is illustrated in Tables 7.4 and 7.5 and will be discussed later.

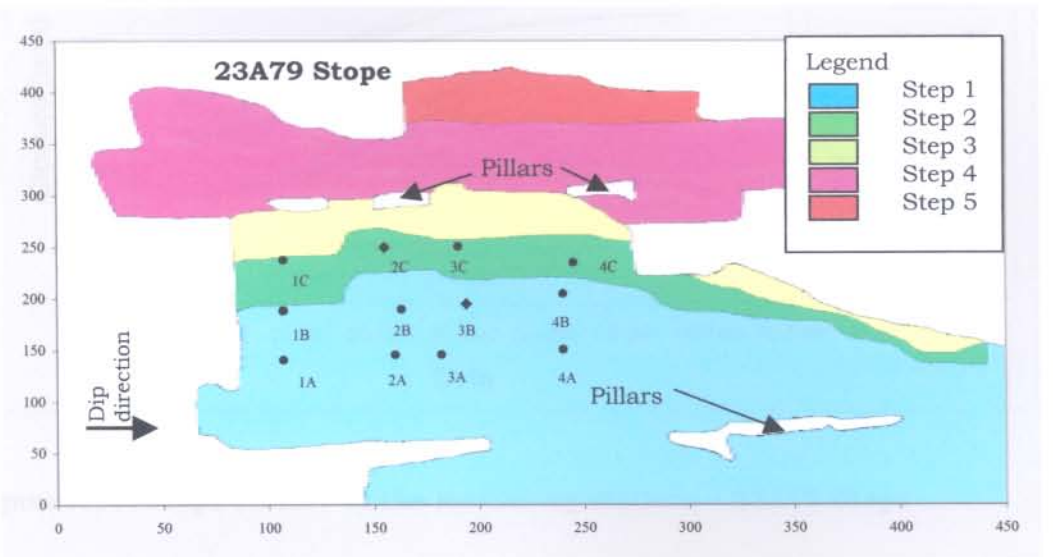

Figure 7.9: Layout and mining steps of the 23A79 Stope

Table 7.4: Summary of closure and closure rates for 23A79 Stope

Date (Mining Stage)	Closure (mm) (Closure rate (mm/day))	Measuring Station										
		1A	1B	1C	2A	2B	2C	3A	3B	3C	4A	4B
2 Oct (A1)		625 *	145 *	* *	695 *	310 *	* *	490 *	* *	* *	520 *	* *
2 Nov (A2)		675 (1.7)	170 (0.8)	* *	775 (2.7)	406 (3.2)	710 *	587 (3.2)	750 *	387 *	680 (5.3)	426 *
5 Dec (A3)		702 (0.8)	190 (0.6)	371 *	887 (3.4)	562 (4.7)	897 (5.7)	708 (3.7)	932 (5.5)	595 (6.3)	823 (4.3)	640 (6.5)
4 Jan (A4)		713 (0.4)	214 (0.8)	399 (0.9)	935 (1.6)	628 (2.2)	975 (2.6)	755 (1.6)	1000 (2.3)	675 (2.7)	874 (1.7)	732 (3.1)
2 Feb (A5)		722 (0.3)	225 (0.4)	410 (0.4)	961 (0.9)	665 (1.3)	1022 (1.6)	778 (0.8)	1034 (1.2)	716 (1.4)	897 (0.8)	777 (1.6)

Where no values are given in the tables below it is due to the fact that the station was either:

* not installed at that stage of mining, or

** was lost.

Figure 7.10: Stope closure at the measuring stations – 23A79 Stope

The stope closures at the different measuring stations for the 23A79 Stope are shown in Figure 7.10. The effect that the regional support has in restricting the magnitude of the closure is illustrated by the fact that the closure rates at the

measuring stations decreases with time. The limiting effect that the regional support has on the stope closure at the measuring stations is evident since the closure tends to asymptotically reach a plateau.

The interaction of the rockmass and the supports used in the 23A79 Stope is illustrated in Figure 7.11. The closure rates given in Table 7.5 were used for the different mining stages, while the number of supports that were used in the analysis was determined from the attributed areas as shown in Table 7.5 and the support standards on the mine. Pencil Props were installed on a grid pattern of 1.5 m on strike by 1.0 m on dip, while the matpacks were installed at 3.0 m centre to centre on all dip and strike gullies. The beam thickness was taken as varying from 7.0 m to 14 m with the increasing mining span and is determined from the Voussoir beam study after Kotzé (1991) as shown in Figure 7.5.

Table 7.5: Attributed areas for measuring stations – 23A79 Stope

Date (Mining Stage)	Measuring Station										
	Attributed area (m^2)	1A	1B	1C	2A	2B	2C	3A	3B	3C	4A	4B
2 Oct (A1)		1814	2040	*	1803	1893	*	1830	*	*	1560	*
2 Nov (A2)		2147	2239	*	2277	2193	2288	2330	2174	1869	2279	1925
5 Dec (A3)		2729	2710	2679	2944	2507	2785	2837	2810	2558	2480	2393
4 Jan (A4)		2913	2836	2899	2968	2969	2864	2944	2968	2869	2730	2802
2 Feb (A5)		2913	2836	2899	2968	2969	2864	2944	2968	2869	2730	2802

The Attributed Areas calculated for all the measuring stations remained the same for the last two mining stages. This comes as a result of the way in which the Attributed Areas are calculated and demonstrates the effect that the presence of the regional support has on the rockmass stiffness that will be calculated from it. The rate of closure at all the measuring stations decreased from the 4th to the 5th stages of mining. It confirms what one would have intuitively expected that the rockmass stiffness should remain almost constant once the regional support starts having a restricting effect of the closure of the area between them.

Figure 7.11 shows the rockmass/support analysis for the 23A79 Stope during the five mining stages (A1 to A5) of mining. This area remained stable even though some of the Pencil Props started to fail some 39 m back from the stope face. No sign of rockmass or stope hangingwall failure was observed during the total extraction of the area. This condition may therefore be described as a stable failure of the stope supports.

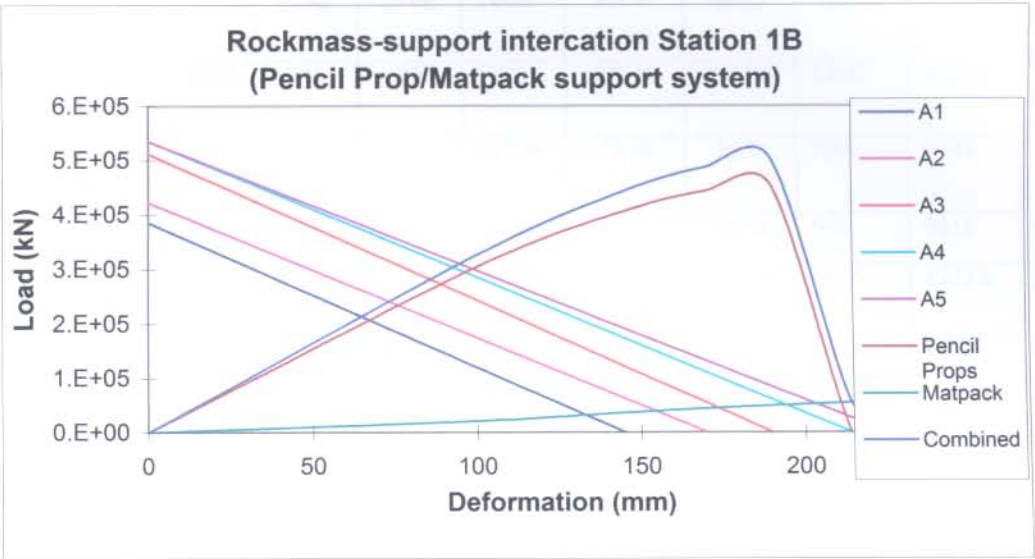

Figure 711: Rockmass and stope support interaction at Station 1B of the 23A79 Stope

(a) Stability analysis summary for station 1B

The rockmass-support interaction is graphically represented in Figure 7.11 while Table 7.6 summarises the stiffness and energy for both the rockmass and supports during the five stages of mining for measuring station 1B.

Table 7.6: Stability analysis summary for Station 1B

Mining Stage	Def. interval (mm)	Stiffness (kN/mm)				Energy (kJ) for mining stage				Comments
		Rock-mass	Supports			Released by rock-mass	Absorbed by the Supports			
			Pencil prop	Mat-pack	Total		Pencil prop	Mat-pack	Total	
A1	0 - 145	-2657	+2801	+202	+3003	27930	34000	1210	35210	*See comments below
A2	145 – 170	-2487	+1483	+226	+1709	1110	8657	766	9423	
A3	170 – 190	-2693	+533	+256	+789	1077	8672	946	9618	
A4	190 – 214	-2503	-18915	+223	-18691	1442	10966	1246	12212	
A5	214 – 250	-2380	0	+198	+198	288	0	614	614	

*Comments:

- Pencil Props start failing 39 m from the stope face that is during mining stage A4.
- Less energy generated by rockmass per mining stage after stage A4 when regional support is established.
- The effect that the regional support has on the energy generated by the rockmass during the 5th mining stage is shown in Table 7.6.
- Pencil Props at this station 1B failing in stage 4 and have failed completely by mining stage A5.
- Matpacks remain stable during all stages of mining.

The stiffness of the rockmass remains negative for all five stages of mining and softens slightly towards the 5th mining stage. The stiffness of the Pencil Props are positive during the first three stages of mining but drastically changed to a strain softening (negative) value during the 4th mining stage. The absolute value of the Pencil Props stiffness is higher than that of the rockmass. This implies that failure of the Pencil Props will take place during the 4th stage of mining. The failure of the Pencil Props explains the increased closure rate during the 3rd mining stage where some of this failure of some of the units could have already started to take place, and the soft matpacks not being able to arrest the closure. The matpacks maintained a positive stiffness during all five stages of mining.

The energy capacity of the supports exceeds that of the rockmass during all five stages of mining even though some of the Pencil Props have failed. This is mainly due to the increased load generated by the matpacks during increased deformation. This condition can therefore be described as stable failure of the supports and explains the fact that the stope remained stable. It also explains the fact that large collapses are arrested by packs that have the capacity to increase their load bearing capacity with increased deformation.

The rockmass behaviour at the particular measuring stations for the two stopes is summarised in Figure 7.12. It shows the five stages of mining and demonstrates that the rockmass stiffness for the 15A47 Stope is much softer than that of the 23A79 Stope for the five stages of mining. It is evident that the pillars in the 23A79 Stope restricted the inelastic deformation of the stope and therefore stiffens the rockmass behaviour as shown in Figure 7.12 below. The influence of the systematic stope pillars on stope closure is clear when comparing the underground closure trends during the five mining stages of the two case studies, i.e. Figures 7.3 and 7.10.

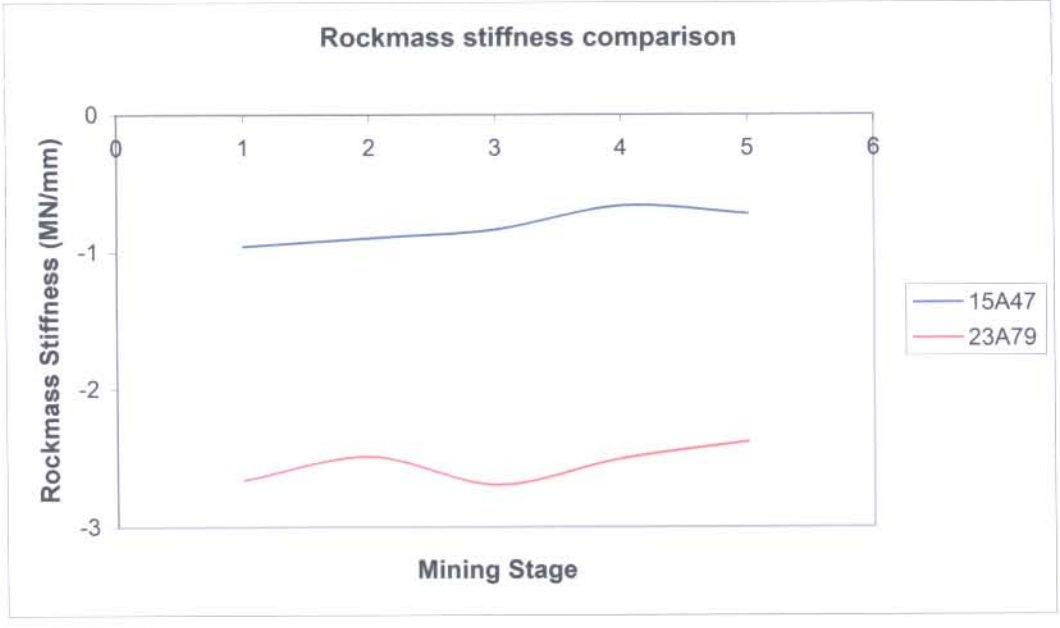

Figure 7.12 Comparison of the rockmass stiffness (MN/mm) for the five mining stages of the two case studies

7.4 CONCLUSION

The applications of the methodology as described in the previous chapters were applied to two case studies at Beatrix Gold Mine. In the first case study unstable failure of the supports occur, while the support in the second case study failed in a stable manner. The in-situ stope support capacity was calculated for the supports of the two case studies, taking into consideration the factors that affect its behaviour.

The rockmass stiffness was also calculated for the different mining stages of the two areas taking into consideration the factors that influence its behaviour such as mining span and geometry, regional support and deformation for the different stages of mining.

The stability analyses that followed from the above where the energy generated and absorbed by the rockmass and support respectively were compared for both case studies. The stiffness of the rockmass and the stope supports were similarly compared as part of the stability analysis. The stable- and unstable failure of the supports that were observed underground is confirmed by this study.

The study shows that the introduction of systematic pillars stiffens the rockmass behaviour by reducing the deformation. This will also reduce the probability for unstable failure of stope support.

REFERENCES

Kotze T.J. (1991). Internal rock engineering report for Beatrix Gold Mine, Gengold, South Africa.

Ozbay M.U. & Roberts M.K.C. (1988). *Yield pillars in stope support* – Proceedings of the first Regional Conference in Africa, South African National Group on Rock Mechanics, Swaziland.

APPENDIX 1

Calculations demonstrating the stability analyses

Working place: **15A47 Stope**

(a) Rockmass

Measuring station:	Station 1
Attributed area:	1884 m^2 (Mining stage A_3)
Mining span:	60 m
Beam thickness (h_t):	8.0 m (from Voussoir beam analysis, Figure 7.5)
Rockmass density (ρ):	2750 kg/m^3
Gravitational acceleration (g):	9.81 m/s^2

The attributed area force (F_o) is given by:

$F_o = \rho.h_t.A_a.g$ (N) where:

F_o = Attributed area force (N);

ρ = Rockmass density (kg/m^3);

h_t = Thickness of hangingwall beam (m);

A_a = Attributed area (m^2); and

g = Gravitational accelaration (m/s^2).

Attributed area force (F_o):	406 605 kN
Deformation interval (mm):	439 – 488 (Mining: stage A_3)
Rockmass stiffness (m):	-833 kN/mm
Rockmass force is described by:	$g(x) = F_o + mx$
	$g(x) = 406\,605 - 833x$ (kN)

Rockmass energy demand (kJ):

Energy demand = $\int_a^b g(x)\partial x = \int_{439}^{488} g(x)\partial x = 1005$ kJ

(b) Stope support system

Type of support: Beatrix Endgrain pack

Support dip spacing (m): 3.0

Support strike spacing (m): 4.0

Stoping width (cm): 145

Support performance function:

$x < 700$ mm: $f(x)_1 = -1683.7x^6 + 3720.9x^5 - 3140.5x^4 + 1282.3x^3 - 266.85x^2 + 33.445x$

$x > 700$ mm: $f(x)_2 = 1956.1x^5 - 2678.8x^4 - 1127.9x^3 + 2899.7x^2 - 1019.8x$

Underground closure rate (mm/day): 1.6

Pack test height (cm): 143

Rate of laboratory test (mm/minute): 30

Load rate factor (Y_f): 0.52

Pack height factor (H_f): 0.98

Pre-stress load (kN): nil

Pack stiffness (kN/mm) at 464 mm deformation:

$\partial/\partial x[f_a(x)] = +2.14$ kN/mm

Support system stiffness (kN/m²): +335.4

Support energy capacity for the deformation interval $439 \leq x \leq 488$ mm

$\int_{439}^{488} f_a(x)\partial x = 95.0$ kJ

Support system energy capacity (kJ): 14911

(c) Comparisons

Stability item	Rockmass	Support system	Comment
Stiffness (kN/mm)	- 833	+ 335	Stable support failure: Support stiffness positive, rockmass stiffness negative.
Energy balance (kJ)	1 005 (Energy demand)	14 911 (Energy capacity)	Stable support failure: Support energy capacity > rockmass demand.